

# Cones and Tubes: Geometry in the Chemistry of Carbon

THOMAS W. EBBESEN\*

ISIS, Louis Pasteur University, 4 rue Blaise Pascal, 67000 Strasbourg, France, and NEC Research Institute, 4 Independence Way, Princeton, New Jersey 08540

Received December 24, 1997

## Introduction

Carbon was believed to be such a well-understood element that the discovery of a whole new class of pure carbon molecules, namely  $C_{60}$  and related fullerenes, at the end of the 20th century caught everyone by surprise.<sup>1,2</sup> After all, carbon in its various forms has been used and studied for centuries. Interestingly,  $C_{60}$  had been around us all the time; it is found in nature and in man-made materials such as in the inks of India or China. Perhaps we did not notice its presence because most of us, but not all,<sup>3</sup> could not readily imagine such structures. Consequently, the impact of  $C_{60}$  has not just been the material itself but the new concepts it has brought to material science and chemistry. Most importantly, it has opened our eyes to the infinite possibility of new structures that can be constructed from simple geometrical principles established by Euler. This is by no means limited to carbon.

If we took the time to look, we would find that nature is displaying such geometrical principles in front of our very eyes. In this regard, probably the best source of inspiration is D'Arcy Thompson's seminal work at the turn of the century, relating biological forms to physical and mathematical laws.<sup>4</sup> Among other things, he noted that *no system of hexagons can enclose space*, and therefore skeletons of living objects made of honeycomb structures had to have units or facets other than hexagons. And indeed they do. On the atomic scale, graphite also has a honeycomb structure. It is composed of a stack of 2-dimensional sheets known as graphene where the  $sp^2$  carbons are arranged in a hexagonal network as shown in Figure 1. So we cannot make any closed structure from graphene such as  $C_{60}$  or a capped nanotube without introducing facets, or rings, other than hexagons. The first part of this Account will be devoted to demonstrating the use of Euler's theorem for lifting graphitic sheets out of

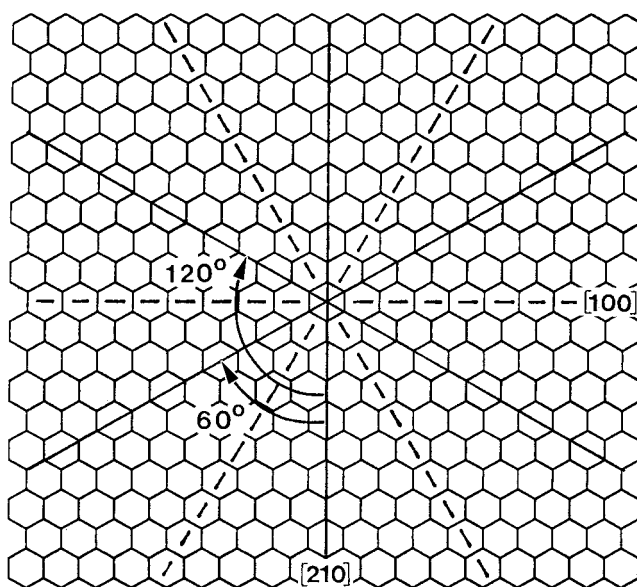


FIGURE 1. Hexagonal network of a single graphite sheet with its symmetry axes.

their 2 dimensions and giving them 3-dimensional closed forms. Through a series of cones, this will naturally lead to nanotubes. Nanotubes illustrate not only the unique properties that can be obtained through novel geometries but also the difficulties of controlling a specific geometry during production. The assembly of new materials in chemistry and supramolecular science could benefit widely from these notions acquired from carbon.

## Graphite in 3 Dimensions

While the number of hexagons in a  $C_{60}$  (20) and a typical closed nanotube ( $\sim 1\,000\,000$ ) are vastly different, they both contain just 12 pentagons. In fact, it does not matter how many hexagons there are, and it does not matter where the pentagons are placed in the hexagonal network (within chemical reason), but one needs at least 12 pentagons to close the structure. This remarkable and simple fact, which comes to light from Euler's theorem, implies that an infinite variety of structures can be made from a graphitic sheet. There are even more options, if rings other than hexagons and pentagons such as heptagons are included, as we shall see next.

Euler's theorem relates the number of vertexes ( $V$ ), edges ( $E$ ), and faces ( $F$ ) of an object as follows:<sup>5–8</sup>

$$V - E + F = X \quad (1)$$

with  $X = 2(1 - g)$ .  $X$  is known as Euler's characteristic and is related to the number of holes  $g$ . For a sphere like  $C_{60}$ ,  $g = 0$ , while for a torus,  $g = 1$ .

For the hexagonal networks of graphite, the  $sp^2$  carbons imply that  $3V = 2E$ , and a more practical expression of

Thomas W. Ebbesen, a physical chemist, was born in Oslo, Norway, in 1954. Upon graduation from a French high school, he took a year off to work as a sailor with thoughts of never opening another chemistry book. He then enrolled at Oberlin College as a biology major, but a course in physical chemistry changed his life. After receiving his Ph.D. from the Curie University in Paris, he worked at the Notre Dame Radiation Laboratory (DOE) before joining NEC Fundamental Research Laboratories in Tsukuba, Japan, in 1988. He became a professor at Pasteur University in Strasbourg in 1996 but continues to hold an appointment at the NEC Research Institute in Princeton, New Jersey.

\* Address correspondence to the author at the NEC Research Institute.

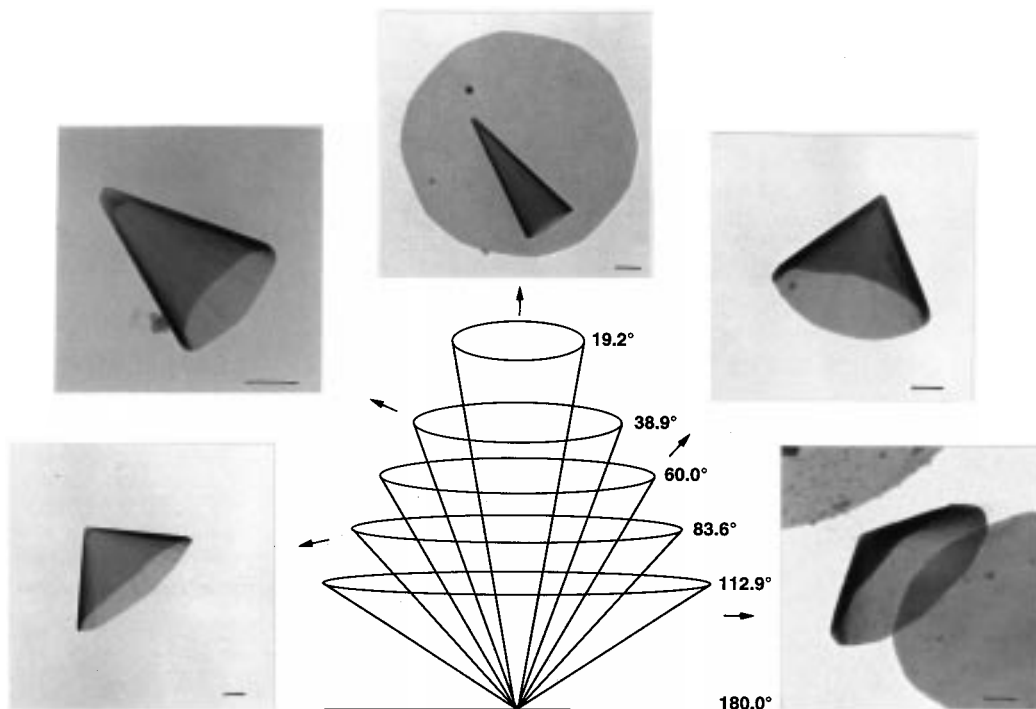


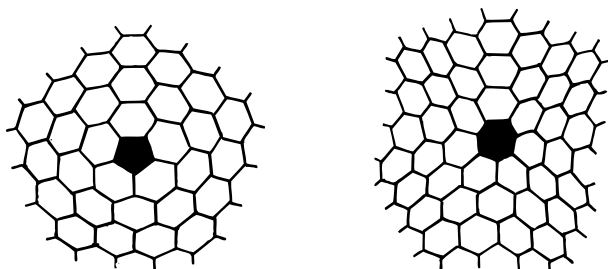
FIGURE 2. Illustration of the five possible graphitic cones<sup>9</sup> and their experimental confirmation<sup>10</sup> (scale bars: 200 nm).

Euler's theorem can be derived:

$$\dots 2n_4 + n_5 - n_7 - 2n_8 \dots = \sum (6 - x)n_x = 12(1 - g) \quad (2)$$

where  $n_x$  is the number of polygons (or rings) having  $x$  sides. Equation 2 is very useful in that it tells how rings, other than hexagons, deform an otherwise flat hexagonal surface and how many are necessary to make a closed structure. A closed structure has a total disclination of  $4\pi$  or  $720^\circ$  (e.g., a sphere). As an example, if  $g = 0$  and if there are no rings other than pentagons ( $n_5$ ), eq 2 gives  $n_5 = 12$ . In other words, 12 pentagons are needed to close the hexagonal network. The disclination produced by each pentagon is therefore equal to  $4\pi/12 = 60^\circ$ . If the structure contains 1 heptagon ( $n_7$ ), then in the absence of other rings, 13 pentagons would be needed to close the structure. In other words, a heptagon produces the opposite disclination of a pentagon ( $-60^\circ$ ), so an extra pentagon is needed to compensate.

In the case of graphene, rings smaller than pentagons  $n_5$  or bigger than  $n_7$  have never been observed, probably for energetic reasons. While the pentagon gives rise to a conical structure, the heptagon produces a saddle-shaped deformation in the hexagonal network:



Graphene has two symmetry directions, namely, the [100] and [210] directions as shown in Figure 1. These repeat every  $60^\circ$  and are offset  $30^\circ$  relative to each other. If one cuts out successively  $60^\circ$  slices along the symmetry axes and reconnects the remaining two edges of the open wedge, one obtains a series of cones.<sup>9,10</sup> The first cone has one pentagon at the apex (a  $60^\circ$  slice was removed from the flat sheet which produced a  $60^\circ$  disclination). The second cone, produced by removing a  $120^\circ$  slice, has a  $120^\circ$  disclination and a square at the apex ( $n_4$ ). However, a cyclobutane-like structure is energetically too costly, so Euler's theorem (eq 2) tells us that it can be replaced by two pentagons ( $2n_5 = n_4 = 120^\circ$  disclination). If we continue this process we find that from a flat graphite sheet we can in the end only make five cones having between one and five pentagons at the apex. These are indeed observed as shown in Figure 2. If we add another pentagon to a "five-pentagon cone", the total disclination is  $2\pi$ , a half-sphere, so that one can expect a cylinder to grow from the edge, as shown in Figure 3.

So with six pentagons, a nanotube is seeded. It will keep growing like a cylinder unless a heptagon or pentagon is accidentally added to the shell.<sup>11,12</sup> A single heptagon will return the cylinder to a conical growth ( $360^\circ - 60^\circ = 300^\circ$ ), as can be seen in Figure 4. Another pentagon will then return the structure to cylindrical ( $300^\circ + 60^\circ = 360^\circ$ ) growth, but notice that the tube is now wider. If we now add another pentagon ( $360^\circ + 60^\circ = 420^\circ$ ), the edges of the structure will grow toward each other and the nanotube will naturally close. In the closing process, another five pentagons must be added in order to leave no dangling bonds and to satisfy Euler's theorem. A variety of nanotube tip structures, including conical ones, have been observed and discussed in detail.<sup>11,12</sup>

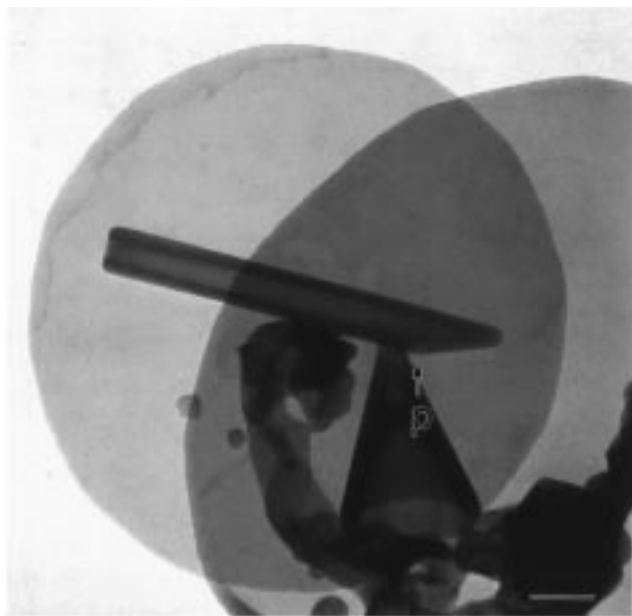


**FIGURE 3.** A five-pentagon cone which changed into a tube upon addition of a sixth pentagon (P) (scale bar: 200 nm). Reprinted with permission from ref 10. Copyright 1997 MacMillan Magazines, Ltd.

We have just seen that Euler's theorem and the material's symmetry govern the formation of 3-dimensional structure from a graphite sheet. There is one other factor which must also be taken into consideration, that is, the ability of graphene to change  $sp^n$  character.<sup>13,14</sup> A flat graphite sheet is pure  $sp^2$ . As soon as it starts curving, it acquires some  $sp^{2+\alpha}$  character. This ability to rehybridize is what gives graphene its out-of-plane flexibility. The rehybridization will, of course, affect the shape and properties of the final structure.<sup>13,14</sup>

While nanotubes are normally grown from seeds having  $360^\circ$  disclinations, the reader will have noticed that a tube can be formed simply by rolling a sheet into a seamless cylinder. The structure is *open* at both ends, and therefore, it has no net disclination. We can use such an open tube to illustrate another very important feature of nanotubes, namely, their chirality.<sup>15</sup> This occurs on the atomic scale and has enormous impact on their electronic properties.<sup>16–21</sup> Starting with an achiral tube (totally symmetric about the long and short axis) as shown in Figure 5a, one can slide the two opposite sides of a line transecting the long axis of the tube until the bonds line up again. At this point the tube is chiral with one, two, or more steps at the growth edge (Figure 5b). One can obtain a variety of chiral tubes by continuing this process.

## Production and Purification of Nanotubes

Nanotubes and other forms of carbon can be produced by various techniques.<sup>20,21</sup> Carbon can form such a variety of products that it is extremely difficult to generate only one geometry, e.g., a nanotube. In addition, even a purified sample contains a distribution of nanotubes having different properties, making interpretation of measurement on bulk samples very difficult.

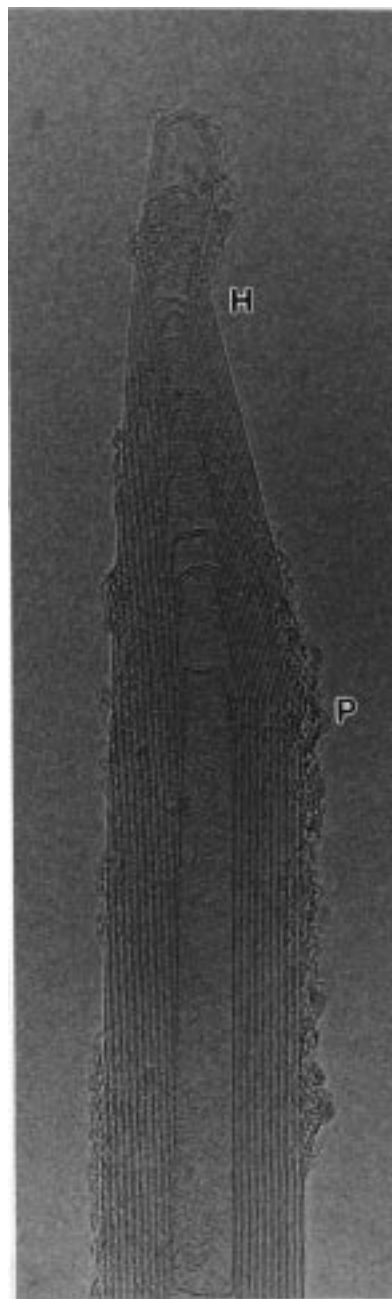


**FIGURE 4.** A multishell nanotube where the successive presence of a heptagon (H) and a pentagon (P) changes the diameter of the structure. The spacing between the concentric layers is ca. 3.4 Å.

For practical purposes, it is useful to distinguish between two types of nanotubes, single-shell (or layer) and multishell tubes. The first nanotubes to be observed were the multishell type.<sup>15</sup> These can be produced in high yields in a carbon arc.<sup>22</sup> This technique yields the best quality multishell tubes (most graphitic and with least defects) because of the high temperature of the arc (4000 K). They always come with about 50% small polyhedral particles, known as nanoparticles, which are similar to well-graphitized small soot particles.<sup>20</sup> Multishell tubes produced catalytically are generally formed at ca. 1300 K from a hydrocarbon precursor and tend to be poorly graphitized. Even annealing this material at high temperature (3000 K) does not produce seamless multishell



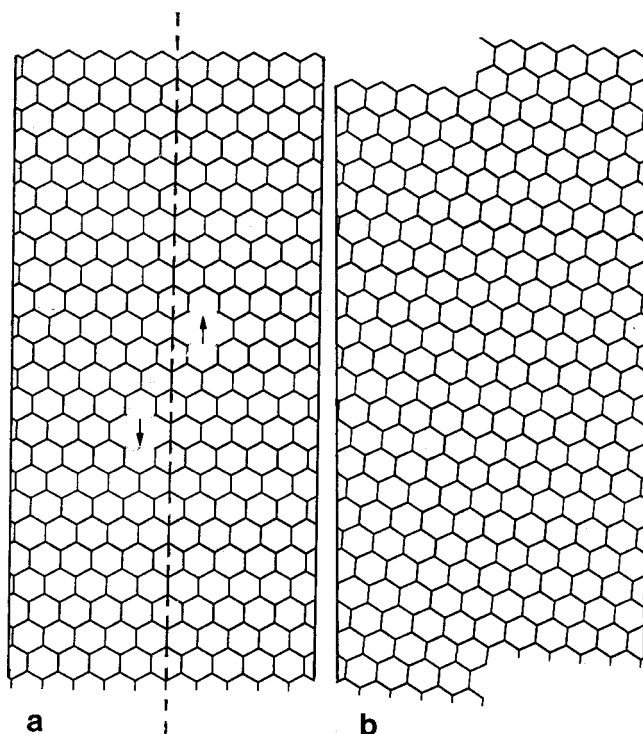


FIGURE 5. A 2-dimensional projection of the transformation of an achiral tube (a) into a chiral one (b) having two steps per turn.

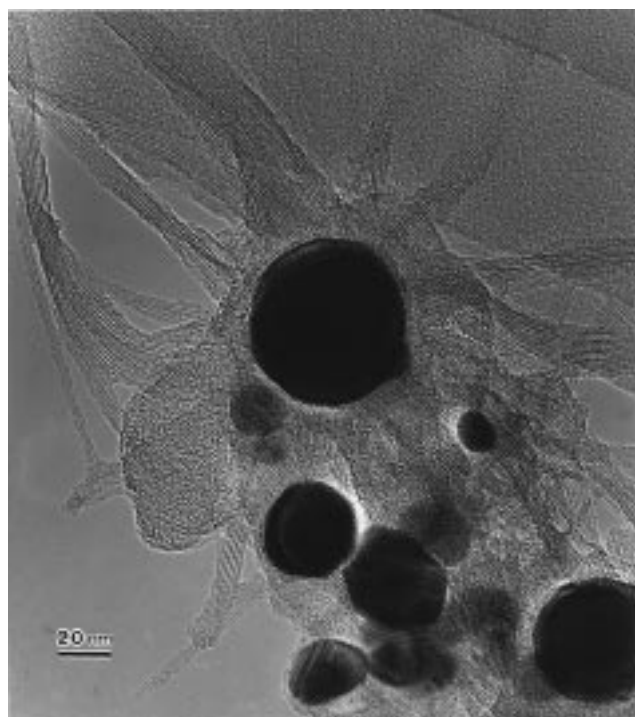


FIGURE 6. Single-shell nanotubes growing radially out from a catalytic particle. Reprinted with permission from ref 38. Copyright 1994 Japanese Journal of Applied Physics.

nanotubes. Therefore, such tubes always have properties that are very far from ideal.

Single-shell nanotubes (Figure 6) were also first found in significant quantities in a carbon arc but in the presence of catalysts (Fe, Co, Ni).<sup>23,24</sup> Later high-yield methods for producing single-shell tubes were developed either using laser ablation of the carbon target in an oven (catalysts:

Ni, Co mixture) or using the carbon arc (catalyst: Ni, Y mixture).<sup>25,26</sup> A variety of single-shell tubes (both chiral and achiral) are produced in these samples under given conditions, and the distribution can be changed, for instance, with the temperature of the oven.

Considering quality, yields, cost, and simplicity, the carbon arc remains the best way of obtaining research quantities (grams) of both single-shell and multishell tubes. The purities of samples tend to be overstated for all the methods. No samples are produced free of contaminants. These include other types of carbon particles, amorphous material, and metals (in the case of the catalytic methods). To purify the samples, there are two categories of techniques, either oxidation<sup>27,28</sup> or separation using surfactants.<sup>29,30</sup> The ease with which these work depends on the types of impurities and the quality of the samples. So the best method must be sought for a given source of samples. Examples of both multishell and single-shell tubes purified by oxidation are shown in Figure 7. For single-shell tubes, a very simple method has recently been developed which eliminates most of the amorphous carbon and dissolves away a significant fraction of the catalytic metals (Figure 7) by reflux in acid.<sup>31</sup>

Nanotubes tend to form bundles due to the strong van der Waals interaction and their high aspect ratio (typically 100–10000).<sup>20,21</sup> This is most visible in the case of the single-shell tubes where they form a closed close-packed arrangement (Figure 7b). Contrary to what was first believed, single-shell nanotubes are not continuous throughout the length of the bundles.<sup>32</sup> So while single-shell nanotubes are known to have a narrow range of diameters centered around 1.2–1.4 nm, their lengths are probably in the micrometer range. Multishell tubes produced in the arc are several micrometers long with inner diameters typically between 1 and 3 nm and out diameters ranging from 2 to 20 nm. Each shell may have a different helicity and therefore different electronic properties.

## Growth Mechanism of Nanotubes and Cones

The formation mechanism of nanotubes and other curved carbon structures, such as fullerenes and soot, in the absence of catalysts is still a big puzzle, of which we know only some of the pieces. Nevertheless, if we combine earlier work on traditional carbon and more recent findings spurred by the renewed interest in carbon, a picture emerges from the fragments.

From studies of carbon blacks, spherical  $sp^2$  carbon particles, we know that the formation of carbon structures involves two stages: seeding (nucleation) and growth.<sup>33</sup> The thermodynamic barrier to nucleation of a structure from the initial carbon “soup” (e.g., carbon plasma) appears to be the limiting step. Carbon cluster studies show that carbon units such as C, C<sub>2</sub>, and C<sub>3</sub> grow into larger linear carbyne chains. As the chains grow longer, they close to form monocyclic rings which are the most

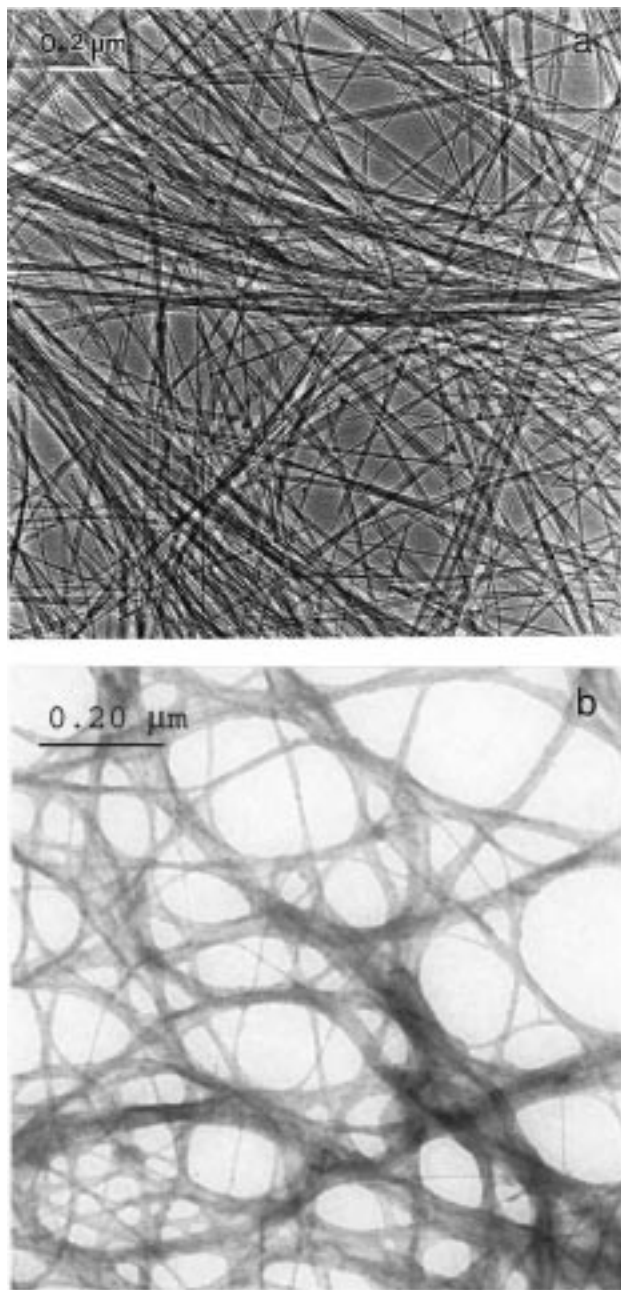


FIGURE 7. Purified multishell (a) and single-shell (b) nanotubes.

stable clusters between ca.  $C_{10}$  and  $C_{36}$ .<sup>34–36</sup> These in turn can undergo interconversions to new structures or coalescence to form larger closed cages such as fullerenes. While there is no question that the monocyclic rings are extremely important precursors to forming curved carbon structures, in a real carbon reactor the situation is rendered more complicated by the continuous supply of new carbon fragments which can react with these rings among other things. This may “freeze” a given monocyclic or other cluster into a configuration with a given disclination.<sup>10</sup> So it is not surprising perhaps that, in a typical experiment, only a small fraction of the recovered soot is  $C_{60}$  (ca. 1%). On the other hand, it is perhaps a wonder that  $C_{60}$  or nanotubes are formed in such high yields considering the numerous reactants, reaction paths, and possible products.

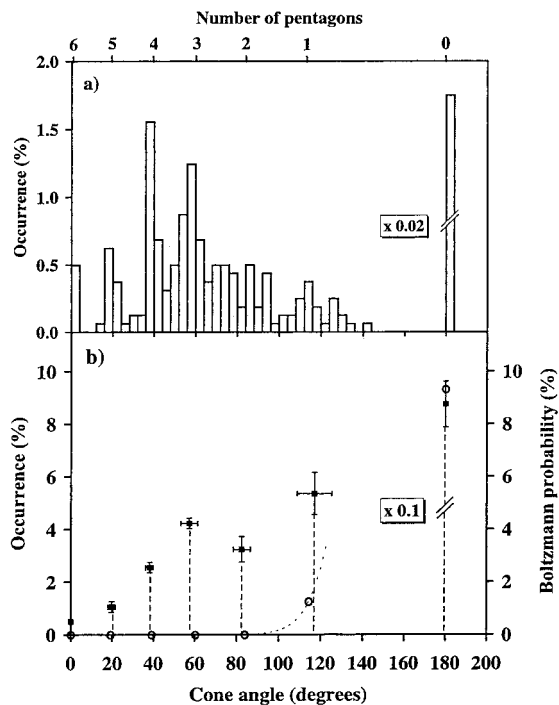


FIGURE 8. (a) Histogram of the measured cone angles in a sample containing disks, cones, and tubes (see Figure 2). (b) Averaged distribution centered at the seven possible disclinations. Reprinted with permission from ref 10. Copyright 1997 MacMillan Magazines, Ltd.

In view of the complexity of sorting out so many parallel reactions, one may ask simpler questions such as what is the probability of seeding a given disclination? Knowing that, can one say something about the final product distribution? Recently we had the chance to look into these questions through an unusual sample produced from passing a hydrocarbon such as heavy oil through a plasma torch.<sup>10</sup> In this sample, each carbon structure has a well-defined and measurable disclination. The sample contains mainly flat disks (no disclination), the five types of cones shown in Figure 2, and nanotubes. In other words, each such domain is representative of a seed having a given disclination multiple of  $60^\circ$ , corresponding to an integer number of pentagons in the structure. By counting the number of each domain type, i.e., making a statistical analysis of the sample, we will find the relative probability of nucleating a given disclination. A total of 1700 domains were counted and measured, and the resulting histogram is shown in Figure 8. We can learn many things from such a histogram.<sup>10</sup> First there are far more domains having a nonzero disclination than expected from simply considering the enthalpy of introducing a pentagon into hexagonal network. Second, it shows a peak at a disclination corresponding to three pentagons at nucleation. Again enthalpy alone cannot account for this result. Therefore, entropy must play a major role in the final product distribution. By entropy, we mean all the possible pathways leading to a given disclination. In other words, starting from the original

carbon plasma soup, there are more paths leading to a cone with 180° disclination than one with a 120° disclination.

The broad distribution of disclinations at nucleation also implies that it will be very difficult to obtain only one type of product such as nanotubes. After seeding, there are both growth along the graphitic planes and the perpendicular thickening of the domain, resulting in multilayer domains such as multishell nanotubes.<sup>20</sup> The introduction of catalysts will of course change the balance and favor certain reaction paths and therefore certain products over others. Thus, one can obtain single-shell tubes in high yields in the presence of catalyst. These grow radially out from the catalytic particles (Figure 6) as has been demonstrated in various studies.<sup>37,38</sup> This is very similar to catalytically grown tubular carbon fibers.<sup>39</sup>

## Properties of Nanotubes

Carbon nanotubes have sparked the imagination of scientists from many different fields due to their unique geometrical features. They have been seen as tiny electric wires, the ultimate fiber for reinforcing other materials, nanoscale chemical reactors, .... While we have been studying many different properties, I will concentrate here on those that are of most interest to chemists and material scientists. The physical properties, in particular the electronic ones, are also fascinating, and the interested reader can find reviews in the literature.<sup>20,21</sup>

**Wetting, Capillarity, and Chemistry.** Nanotubes are not molecules but rather long quasi-1-dimensional microcrystals. For instance, we can only disperse them in solution, not dissolve them. Therefore, if one wishes to study their chemistry, study their blending with a polymer for reinforcement purposes, study the capillarity of their inner cavity, coat the outer surfaces, etc., one needs to understand their wetting properties. The wetting property reflects the interactions between the nanotube surface and a liquid relative to the cohesive forces in the liquid. If a droplet is placed on a surface, it will take a shape which directly reflects the relative strength of these two interactions. The tangent at the contact point forms an angle known as the contact angle  $\theta$ : If the contact angle is  $<90^\circ$ ,



the liquid is considered to be wetting, while if it is  $>90^\circ$ , it is said to be nonwetting. The reason for this nomenclature can be easily understood from the Laplace equation which relates capillarity to wetting:<sup>40,41</sup>

$$\Delta P = (2\gamma \cos \theta)/r \quad (3)$$

where  $\Delta P$  is the pressure difference across the meniscus,  $r$  the radius of curvature, and  $\gamma$  the surface tension of the liquid (at the liquid–vapor interface). If  $\theta > 90^\circ$ ,  $\cos \theta$  becomes negative and therefore so does  $\Delta P$ . In other words, a nonwetting angle implies that an external pressure (greater than  $\Delta P$ ) must be applied to force the liquid

**Table 1. Wetting Properties of Multishell Nanotubes as a Function of the Surface Tension of Various Substances**

substance	$\gamma$ (mN/m)	wetting	substance	$\gamma$ (mN/m)	wetting
HNO <sub>3</sub>	43	yes	Te	190	no
S	61	yes	Pb	470	no
Cs	67	yes	Hg	490	no
Se	97	yes	Ga	710	no

into the capillary. Conversely, if  $\theta < 90^\circ$ ,  $\Delta P$  is positive, and the liquid will spontaneously be sucked into a hollow cavity by the capillary action.

It is very hard to predict wetting or the contact angle which itself is given by

$$\cos \theta = (\gamma_{SV} - \gamma_{SL})/\gamma \quad (4)$$

where  $\gamma_{SV}$  and  $\gamma_{SL}$  are the tensions at the solid–vapor and solid–liquid interfaces. In addition, the Laplace equation was designed for macroscopic systems, and it is not definite that it holds on the nanometer scale.<sup>42,43</sup>

Experimentally, the way around this problem is to remember that since wetting is a necessary condition to observe capillarity, capillarity can in turn be used to evaluate wetting (i.e., if  $\theta < 90^\circ$  or not).<sup>41</sup> For that one does not even need open tubes as the space between closed packed tubes will act as capillaries. So the wetting properties of nanotubes are determined by placing a powder of a given material on top of nanotubes packed in the bottom of a test tube. Then it is heated under vacuum to the melting temperature of the substance to be tested. When the powder melts, either it is sucked into the nanotube matrix (wetting,  $\theta < 90^\circ$ ) or it forms a ball on top of the nanotubes, like mercury on glass, indicating nonwetting. In Table 1 are listed the results as a function  $\gamma$ . One can immediately see that there is a cutoff in terms of surface tension above which no wetting occurs whatever the chemical nature of the wetting substance. Using open nanotubes, one can verify that the inside will indeed be filled by low surface tension substances as shown in Figure 9.<sup>41</sup>

A higher polarizability of the solid substrate versus the liquid is important for wetting.<sup>35</sup> The cutoff around 190 mN/m is an average, and it is expected to vary with the helicity and diameter of the tubes since these affect their electronic properties and therefore the polarizability. Calculations have shown that the wetting properties of extremely thin ( $<1$  nm) single-shell tubes might be very different.<sup>43</sup> However, such small tubes are very rare in normal samples.

Using the knowledge of the wetting properties of nanotubes, one can explain why nanotubes were first observed to be filled through capillary action by lead and bismuth oxides<sup>44,45</sup> since they both have low surface tensions.<sup>20,21</sup> It is also clear that nanotubes cannot be filled with the high surface tension metals by capillary action.

The fact that nanotubes are wet by low surface tension liquids portends well for chemistry since organic solvents all fall in that category. It is also known that nanotubes oxidize from the tip inward, layer by layer,<sup>45,46</sup> eventually leaving the tubes open at the ends. A simple and elegant



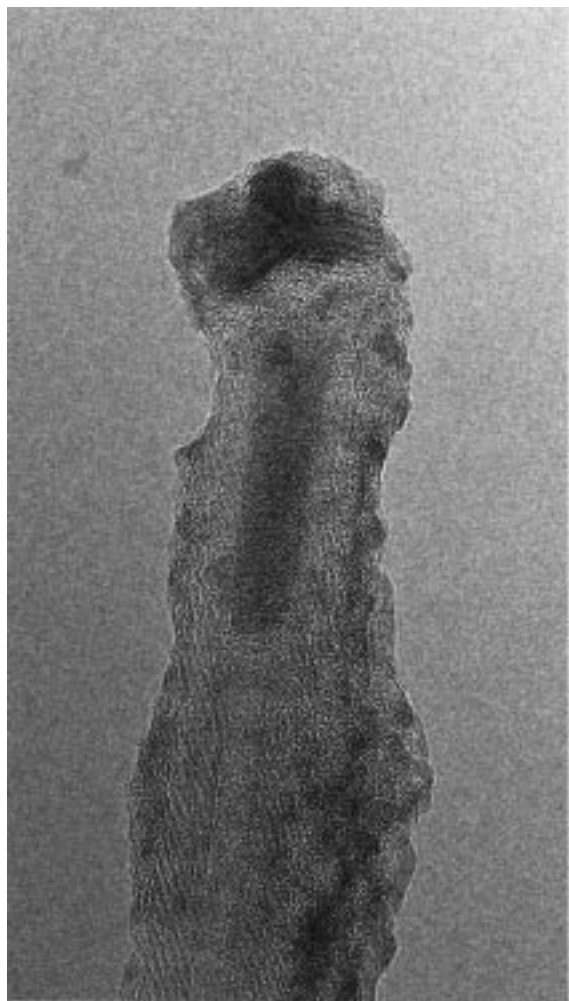


**FIGURE 9.** A multishell filled with Se by capillary action. Reprinted with permission from ref 41. Copyright 1994 American Association for the Advancement of Science.

method has been developed to fill multishell nanotubes which plays on both of these properties.<sup>47</sup> Nitric acid will oxidize the tips of nanotubes but then be pulled in by capillary action, the surface tension being only 43 mN/m. If compounds, such inorganic salts, are dissolved in the acid, they will enter the tube together. In other words, the nitric acid acts not only as an oxidant for opening the tubes but also as a low surface tension carrier. Filling single-shell nanotubes by such methods appears to be difficult simply because the inner cavity is so small (ca. 10 Å) that a few oxide groups at the entrance might sterically hinder the entry of any molecule or element.

There is actually little known about the chemistry of nanotubes except for oxidation.<sup>45–47</sup> While the chemistry of C<sub>60</sub> is dominated by the “pyracylene” unit (two pentagons separated by a double bond),<sup>48</sup> the pentagons on nanotubes are typically very far apart so one cannot expect to find such reactivity. Even if the pentagons provide reaction sites, there are only six on each end of a very long structure containing millions of atoms. So shorter tubes or the development of general surface reactions is necessary for better functionalization.

For instance, oxidation of multishell nanotubes, either by acids or in air at ca. 700 °C, can be used as an initiation

point for further chemical modification since it leaves the surface of multishell tubes covered with three types of functional groups: –COOH, –COH, and –C=O in a ratio of roughly 4:2:1.<sup>49</sup> Not surprisingly, the oxidized nanotubes disperse much better in polar solvents. Oxidized nanotubes may also provide a better anchoring in host polymers as discussed in the next paragraph. Single-shell tubes would probably fall apart as the walls become entirely covered with oxides. However, if they were broken up using sonication like multishell tubes,<sup>50</sup> then the smaller units should provide more reactive sites per unit length. For those who might dream of making small metallic or semiconductive units by such an approach, it must be remembered that as the nanotube becomes shorter and shorter the electronic structure will change, eventually leaving only the typical molecular features with large HOMO–LUMO gaps and colorful tubes.

**Mechanical Properties.** Large carbon fibers are already used for reinforcing other materials in sporting goods and aerospace industry due to their strength and their low density. It is known that the fibers become stronger as the graphite sheets are more aligned with the long axis of the fiber.<sup>51</sup> Graphite sheets are the strongest material in-plane, but they easily undergo out-of-plane deformations<sup>13,14</sup> due to the ability of the atoms to rehybridize (hence the “softness” of graphite). Therefore, seamless nanotubes with their continuous graphitic sheets were expected to be the ultimate fiber as far as mechanical strength is concerned. Moreover, nanotubes easily meet the criteria of having diameters less than 0.1 μm and aspect ratios larger than 20 which are considered ideal for reinforcement purposes.<sup>52</sup>

So how strong are carbon nanotubes? When nanotubes are bent beyond a certain point, they start to buckle and deform. Experiments and calculations show that the nanotubes will recover from even more severe deformations.<sup>20,53,54</sup> In other words, nanotubes have elastic character, and unlike graphene, they do not easily tear. At the same time, the nanotubes resist bending due to the inherent strength of the carbon–carbon bonds reflected in Young’s modulus.

Measuring Young’s modulus of nanotubes was a real challenge as one could not very well just put tweezers on each end and pull! We found another approach which should be useful for all nanoscopic materials. In the transmission electron microscope, TEM, we can see nanotubes vibrate due to thermal energy when they are just clamped down at one end (Figure 10).<sup>55</sup> The mean-square amplitude of this vibration  $\sigma^2$  is directly proportional to the thermal energy  $kT$  and inversely proportional to Young’s modulus  $Y$ , as follows:<sup>55</sup>

$$\sigma^2 = \frac{0.4243 L^3 kT}{Y(a^4 - b^4)} \quad (5)$$

where  $L$  is the free-standing length and  $a$  and  $b$  are the outer and inner diameters of the tube. A plot of  $\sigma^2$  versus  $T$  gives indeed a straight line whose slope yields  $Y$ . The average Young’s modulus value was found to be  $\sim 1.8$  TPa

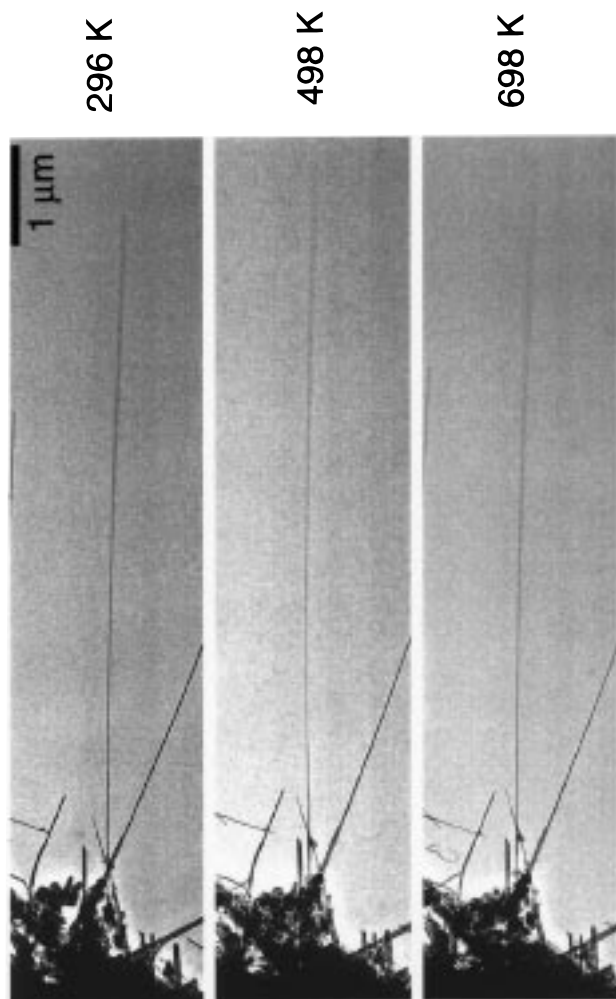


FIGURE 10. Multishell tubes vibrating at different temperatures. Notice the increasing bluriness at the tips.<sup>55</sup> Courtesy of M. M. J. Treacy.

for multishell tubes. More recently, a value of  $\sim 1.3$  TPa was found using a different technique.<sup>56</sup> These values are the highest of any known material and higher than that of graphite (the best estimate is  $>1.09$  TPa) which is presently hard to justify unless the value of graphite is higher than currently reported. As the diameters of the tubes become smaller, such as those of single-shell tubes, theoretical studies have predicted both higher and lower Young's modulus than graphite.<sup>54,57</sup> Further experiments are necessary to clarify this point.

Since nanotubes are wet by low surface tension liquids, they should mix well with polymers in the liquid phase. The strength of the interaction in the final solidified phase might still not be sufficient for transferring all the strength of the nanotubes to the host polymer. One example shows that the nanotubes are indeed well dispersed in an epoxide matrix.<sup>58</sup> However, when the reinforced polymer was cut, the nanotubes slid out of the matrix, indicating the need for further anchoring the tubes through chemical modification. Oxidized tubes might provide the simplest answer to this problem.

## Implications

While there has been much accomplished in our understanding of novel carbon materials over the past decade, much still needs to be done. In particular, their nucleation and growth need further study to achieve control of the products formed. The ultimate goal is to tailor carbon to a desired property by controlling its geometry. The chemistry and material science of nanotubes are still in their infancy, and much can be learned from traditional carbon materials. On the other hand, our understanding of established carbon materials can benefit enormously from the concepts implicit in the newer ones.

The novel carbon structures are perhaps the clearest example of the use of simple geometrical laws such as Euler's theorem to construct a great variety of structures from a given element. This has already been extended to other materials, such as  $\text{MoS}_2$ ,  $\text{WS}_2$ , and  $\text{BN}$ .<sup>59–61</sup> In an age when there is so much interest in building large molecular and supramolecular structures, it would seem that Euler's theorem could also be used to achieve a variety of 3-dimensional molecular structures from a few simple subunits. Such "eulerenes", of which fullerenes would be the pure carbon subgroup,<sup>62</sup> could form a whole new class of compounds constructed from modules where geometry, properties, and function would be intimately linked. This should be within reach of today's synthetic chemists.

## References

- (1) Kroto, H. W.; Heath, J. R.; O'Brien, S. C.; Curl, R. F.; Smalley, R. E. *Nature* **1985**, *318*, 162.
- (2) Kratschmer, W.; Lamb, L. D.; Fostiropoulos, K.; Huffman, D. R. *Nature* **1990**, *347*, 354.
- (3) See for example: Jones, D. E. H. *New Sci.* **1966**, *32*, 245. Osawa, E. *Kagaku (Kyoto)* **1970**, *25*, 854 (in Japanese). Bochvar, D. A.; Gal'pern, E. G. *Dokl. Akad. Nauk SSSR* **1973**, *209*, 610 (in Russian). Davidson, R. A. *Theor. Chim. Acta* **1981**, *58*, 193.
- (4) Thompson, D'Arcy W. *On Growth and Form*; Cambridge University Press: Cambridge, 1969.
- (5) Terrones, H.; Mackay, A. L. *Carbon* **1992**, *30*, 1251.
- (6) Terrones, H.; Terrones, M.; Hsu, W. K. *Chem. Soc. Rev.* **1995**, 341.
- (7) Dunlap, B. I. *Phys. Rev. B* **1994**, *49*, 5643.
- (8) Osawa, E.; Yoshida, M.; Fujita, M. *MRS Bull.* **1994**, *19*, 33.
- (9) Ge, M.; Sattler, K. *Chem. Phys. Lett.* **1994**, *220*, 192.
- (10) Krishnan, A.; Dujardin, E.; Treacy, M. M. J.; Hugdahl, J.; Lynum, S.; Ebbesen, T. W. *Nature* **1997**, *388*, 451.
- (11) Iijima, S.; Ichihashi, T.; Ando, Y. *Nature* **1992**, *356*, 776.
- (12) Ajayan, P. M.; Ichihashi, T.; Iijima, S. *Chem. Phys. Lett.* **1993**, *202*, 384.
- (13) Hiura, H.; Ebbesen, T. W.; Fujita, J.; Tanigaki, K.; Takada, T. *Nature* **1994**, *367*, 148.
- (14) Haddon, R. C. *Science* **1993**, *261*, 1545.
- (15) Iijima, S. *Nature* **1991**, *354*, 56.
- (16) Mintmire, J. W.; Dunlap, B. I.; White, C. T. *Phys. Rev. Lett.* **1992**, *68*, 631.
- (17) Hamada, N.; Sawada, S.; Oshiyama, A. *Phys. Rev. Lett.* **1992**, *68*, 1579.
- (18) Saito, R.; Fujita, M.; Dresselhaus, G.; Dresselhaus, M. S. *Appl. Phys. Lett.* **1992**, *60*, 2204.
- (19) White, C. T.; Robertson, D. H.; Mintmire, J. W. *Phys. Rev. B* **1993**, *47*, 5485.



- (20) Ebbesen, T. W., Ed. *Carbon Nanotubes: Preparation and Properties*; CRC Press: Boca Raton, FL, 1997.
- (21) Ajayan, P. M.; Ebbesen, T. W. *Rep. Prog. Phys.* **1997**, *60*, 1025.
- (22) Ebbesen, T. W.; Ajayan, P. M. *Nature* **1992**, *358*, 220.
- (23) Iijima, S.; Ichihashi, T. *Nature* **1993**, *363*, 603.
- (24) Bethune, D. S.; Kiang, C. H.; de Vries, M. S.; Gorman, G.; Savoy, R.; Vazquez, J.; Beyers, R. *Nature* **1993**, *363*, 605.
- (25) Guo, T.; Nikolaev, P.; Thess, A.; Colbert, D. T.; Smalley, R. E. *Chem. Phys. Lett.* **1995**, *243*, 49.
- (26) Journet, C.; Maser, W. K.; Bernier, P.; Loiseau, A.; Lamy de la Chapelle, M.; Lefrant, S.; Deniard P.; Lee, R.; Fischer, J. E. *Nature* **1997**, *388*, 756.
- (27) Ebbesen, T. W.; Ajayan, P. M.; Hiura, H.; Tanigaki, K. *Nature* **1994**, *367*, 519.
- (28) Chen, Y. K.; Green, M. L. H.; Griffin, J. L.; Hammer, J.; Lago, R. M.; Tsang, S. C. *Adv. Mater.* **1996**, *8*, 1012.
- (29) Bonard, J.-M.; Stora, T.; Salvétat, J.-P.; Maier, F.; Stockli, T.; Duschl, C.; Forro, L.; de Heer, W. A.; Chatelain, A. *Adv. Mater.* **1997**, *9*, 827.
- (30) Bando, S.; Rao, A. M.; Williams, K. A.; Thess, A.; Smalley, R. E.; Eklund, P. C. *J. Phys. Chem. B* **1997**, *101*, 8839.
- (31) Dujardin, E.; Ebbesen, T. W.; Krishnan, A.; Tracey, M. M. *J. Adv. Mater.* **1998**, *10*, 611.
- (32) P. Bernier, private communication.
- (33) Lahaye, J.; Prado, G. In *Particulate Carbon*; Sieglä, D. C., Smith, G. W., Eds.; Plenum Press: New York, 1981; p 33.
- (34) McElvany, S. W.; Ross, M. M.; Goroff, N. S.; Diederich, F. *Science* **1993**, *259*, 1594.
- (35) Hunter, J.; Fye, J.; Jarrold, M. F. *J. Phys. Chem.* **1993**, *97*, 3460.
- (36) Heath, J. R. In *Fullerenes: Synthesis, Properties, and Chemistry of Large Carbon Clusters*; Hammond, G. S., Kuck, V. J., Eds.; American Chemical Society: Washington, DC, 1991; pp 1–23.
- (37) Subramoney, S.; Ruoff, R. S.; Lorents, D. C.; Malhotra, R. *Nature* **1993**, *366*, 637.
- (38) Saito, Y.; Okuda, M.; Fujimoto, N.; Yoshikawa, T.; Tomita, M.; Hayashi, T. *Jpn. J. Appl. Phys.* **1994**, *33*, L526.
- (39) Oberlin, A.; Endo, M.; Koyama, T. *J. Cryst. Growth* **1976**, *32*, 335.
- (40) Adamson, A. W. *Physical Chemistry of Surfaces*; John Wiley & Sons: New York, 1990.
- (41) Dujardin, E.; Ebbesen, T. W.; Hiura, H.; Tanigaki, K. *Science* **1994**, *265*, 1850.
- (42) de Gennes, P. G. *Rev. Mod. Phys.* **1985**, *57*, 827.
- (43) Miyamoto, Y.; Rubio, A.; Blase, X.; Cohen, M. L.; Louie, S. G. *Phys. Rev. Lett.* **1995**, *74*, 2993.
- (44) Ajayan, P. M.; Iijima, S. *Nature* **1993**, *361*, 333.
- (45) Ajayan, P. M.; Ebbesen, T. W.; Ichihashi, T.; Iijima, S.; Tanigaki, K.; Hiura, H. *Nature* **1993**, *362*, 522.
- (46) Tsang, S. C.; Harris, P. J. F.; Green, M. L. H. *Nature* **1993**, *362*, 520.
- (47) Tsang, S. C.; Chen, Y. K.; Harris, P. J. F.; Green, M. L. H. *Nature* **1994**, *372*, 159.
- (48) Wudl, F. *Acc. Chem. Res.* **1992**, *25*, 157.
- (49) Ebbesen, T. W.; Hiura, H.; Bisher, M. E.; Treacy, M. M. J.; Shreeve-Keyer, J. L.; Haushalter, R. C. *Adv. Mater.* **1996**, *8*, 155.
- (50) Lu, K. L.; Lago, R. M.; Chen, Y. K.; Green, M. L. H.; Harris, P. J. F.; Tsang, S. C. *Carbon* **1996**, *34*, 814.
- (51) Dresselhaus, M. S.; Dresselhaus, G.; Sugihara, K.; Spain, I. L.; Golberg, H. A. *Graphite Fibers and Filaments*; Springer-Verlag: Berlin, 1988.
- (52) Calvert, P. *Nature* **1992**, *357*, 265.
- (53) Falvo, M. R.; Clary, G. J.; Taylor, R. M., II; Chi, V.; Brooks, F. P., Jr.; Washburn, S.; Superfine, R. *Nature* **1997**, *389*, 582.
- (54) Yakobson, B. I.; Brabec, C. J.; Bernholc, J. *Phys. Rev. Lett.* **1996**, *76*, 2511.
- (55) Treacy, M. M. J.; Ebbesen, T. W.; Gibson, J. M. *Nature* **1996**, *381*, 678.
- (56) Wong, E. W.; Sheehan, P. E.; Lieber, C. M. *Science* **1997**, *277*, 1971.
- (57) Robertson, D. H.; Brenner, D. W.; Mintmire, J. W. *Phys. Rev. B* **1992**, *45*, 12592.
- (58) Ajayan, P. M.; Stephan, O.; Colliex, C.; Trauth, D. *Science* **1994**, *265*, 1212.
- (59) Tenne, R.; Margulis, L.; Genut, M.; Hodes, G. *Nature* **1992**, *360*, 444.
- (60) Redlich, Ph.; Loeffler, J.; Ajayan, P. M.; Bill, J.; Aldinger, F.; Ruhle, M. *Chem. Phys. Lett.* **1996**, *260*, 465.
- (61) Chopra, N. G.; Luyken, R. J.; Cherrey, K.; Crespi, V. C.; Cohen, M. L.; Louie, S. G.; Zettl, A. *Science* **1995**, *269*, 966.
- (62) The definition of a fullerene follows: "Fullerenes are defined as polyhedral closed cages made up entirely of n three-coordinate carbon atoms and having 12 pentagonal and (n/2–10) hexagonal faces, where n is greater than or equal to 20. Other polyhedral closed cages made up entirely of n three-coordinate carbon atoms shall be known as quasi-fullerenes." Private communication, Roger Taylor.

AR960168I